Application of Time-Dependent Density-Functional Theory to Electron–Ion Coupling in Ethylene

GEORGE F. BERTSCH,[a,*] JEFFREY GIANSIRACUSA,[a] AND KAZUHIRO YABANA[b]
[a]Department of Physics and Institute for Nuclear Theory, Box 351560, University of Washington, Seattle, Washington 98915, USA
[b]Institute of Physics, University of Tsukuba, Tsukuba 305-8571, Japan

(Received 7 October 2002 and in revised form 15 December 2002)

Abstract. To examine the applicability of the time-dependent density-functional theory (TDDFT) for treating the electron–nucleus coupling in excited states, we calculate the strength distribution associated with the π–π* transition in ethylene. The observed optical transition strength in the 7–8.5 eV region shows a complex structure arising from coupling to C–C stretch motion, to torsional motion, and to Rydberg excitations. The mean energy of the observed peak is reproduced to about 0.2 eV accuracy by the TDDFT in the local density approximation (LDA). The reflection approximation is used to calculate the peak broadening. Roughly half of the broadening can be attributed to the fluctuation in the C–C coordinate. The asymmetry in the line shape is also qualitatively reproduced by the C–C coordinate fluctuation. We find, in agreement with other theoretical studies, that the torsional motion is responsible for the progression of weak transition strength extending from the peak down to about 6 eV. The LDA reproduces the strength in this region to a factor of about 3. We conclude that the TDDFT is rather promising for calculating the electron–nucleus coupling at short times.

1. INTRODUCTION

The time-dependent density-functional theory (TDDFT) offers a compromise between economy and accuracy for the calculation of electronic excitations in atoms, molecules, and condensed matter. The electronic excitation energies are typically reproduced by a few tenths of an electronvolt for states with large oscillator strengths, and their strengths are typically reproduced within 25% accuracy.[1,2] We are now interested in seeing how much further the theory can be applied at this level of accuracy and, in particular, how well it works in describing the coupling of electronic excitations to the nuclear degrees of freedom.

In a previous publication, we examined this question taking the benzene molecule for a case study.[3] There we found that the TDDFT worked rather well at describing the nominally forbidden transitions, reproducing oscillator strength over 3 orders of magnitude with errors at the 30% level. Besides giving transition strength to the symmetry-forbidden transitions, the electron–nucleus coupling induces a vibrational splitting of each electronic line. While the detailed description requires the Franck–Condon factors of the individual vibrational states, the overall widths can be calculated with much simpler theory. For benzene, we found that the overall widths associated with the vibrational splittings were reproduced within 25% accuracy.

Ethylene is an even simpler molecule whose absorption spectrum has been subject to much theoretical study by the methods of quantum chemistry. The observed photoabsorption spectrum in ethylene shows a strong, structured peak in the region of 7–8.5 eV excitation that may be largely attributed to the π–π* transition. The studies of refs 4 and 5 present detailed calculations of

*Author to whom correspondence should be addressed. E-mail: bertsch@mocha.phys.washington.edu

the vibronic couplings, but they do not make a direct comparison to experiment. We also note the calculations by Ben-Nun et al.,[6] in which the subsequent nuclear motion is treated quantum mechanically. The goal of the present article is less ambitious: We aim to see how well the density-functional theory (DFT) works for electron–nucleus coupling at short times, before the system responds dynamically. We will focus on the π–π^* transition, which is of general interest for the optical properties of conjugated carbon systems.

The basic properties of the transition, besides its mean energy, are its width (about 1 eV FWHM) and its oscillator strength, measured to be $f = 0.42$.[7] A feature of particular interest is the long progression of strength on the low-energy side of the peak, extending down to about 6 eV. We shall also apply the TDDFT to this feature and directly compare the theoretical and the experimental strength in the region of 6–7 eV.

2. CALCULATIONAL METHOD

We use the DFT to calculate the ground potential energy surface (PES) as well as the excited PES. In the present work, we use a simple density-functional based on the local density approximation (LDA).[8]

Denoting the nuclear coordinates by Q, the ground PES $E_{gs}(Q)$ is obtained in the static theory by minimizing the energy functional of the orbital variables. The optimized orbitals ϕ_i satisfy the Kohn–Sham equations

$$-\frac{\nabla^2}{2m}\phi_i + \frac{\delta \mathcal{E}}{\delta n}\phi_i = \epsilon_i \phi_i \tag{1}$$

Here $\mathcal{E}$ is the energy functional including Coulomb interactions but not including the electrons' orbital kinetic energy.

The excited states are calculated by solving the linearized equations of the TDDFT. These equations are very close to the RPA (Random Phase Approximation) equations, differing only by the presence of an exchange-correlation term in the interaction. For each ground-state orbital ϕ_i, there are two excited wave functions, ϕ_i^+ and ϕ_i^-. The equations they satisfy are

$$-\frac{\nabla^2}{2m}\phi_i^\pm + \frac{\delta \mathcal{E}}{\delta n}\phi_i^\pm - \epsilon_i \phi_i^\pm + \frac{\delta^2 \mathcal{E}}{\delta n^2}\delta n \phi_i = (\epsilon_i \pm \omega)\phi_i^\pm$$

with the normalization condition, $\langle \phi_i^+ | \phi_i^+ \rangle - \langle \phi_i^- | \phi_i^- \rangle = 1$. The physical quantities extracted from the solutions are the eigenvalues ω, representing vertical excitation energies, and the transition densities $\delta n = \Sigma_i \phi_i (\phi_i^+ + \phi_i^-)$, which represent the matrix elements of the density operator between the ground and the excited states. The excited PES is given by the sum of the ground PES and the excitation energy ω,

$$E_{ex}(Q) = E_{gs}(Q) + \omega(Q) \tag{2}$$

To describe the oscillator strength distribution, we treat nuclear motion classically except for the zero-point motion on the ground PES. This is called the reflection approximation.[9,10] Also, we neglect couplings between different vibrational degrees of freedom and treat the fluctuations in various coordinates Q independently. The reflection formula for the strength function is

$$\frac{df}{dE} = f(Q)\left(\frac{dE_{ex}}{dQ}\right)^{-1} |\Psi(Q)|^2 \tag{3}$$

where the coordinate Q in this expression is obtained by inverting the equation $E = E_{ex}(Q)$. In the formula, $\Psi(Q)$ denotes the vibrational nuclear wave function in the ground PES, normalized as $\int |\Psi|^2 dQ = 1$. Also $f(Q)$ denotes the oscillator strength at a fixed Q between the ground and the excited state. In ref 3, we used an even simpler approximation, namely, taking the vibrations to be harmaonic and treating other factors in eq 3 as constant. Then the width is Gaussian with an energy variance σ_E given by

$$\sigma_E = \left.\frac{dE_{ex}}{dQ}\right|_0 \sigma_Q \tag{4}$$

where σ_Q is the variance of Q in the ground-state vibrational wave function. For a Gaussian profile, the variance is related to the width Γ by $\Gamma = 2.3\sigma_E$.

Our computational method is quite different from usual quantum chemistry methods in that we employ a three-dimensional Cartesian grid representation for the orbital wave functions. Only valence electrons are explicitly included in the functional. More tightly bound electrons are taken into account by pseudopotentials constructed with a commonly used prescription.[11,12] Further details on the computation may be found in our previous publications, e.g.[1] The important numerical parameters in the computations are the mesh spacing Δx and the shape and size of the volume on which the grid is defined. In our previous work on conjugated carbon systems, we used a grid spacing of $\Delta x = 0.3$ Å. With that mesh, orbital energies are converged to better than 0.1 eV. One can use the same coarse mesh to compute the coupling to the vibrational degrees of freedom, provided the ground PES is independently known. In ref 3 we only considered small amplitudes of nuclear motion, obtaining the necessary information from empirical data on the vibrations. Here we want to consider larger amplitudes of motion, beyond the harmonic regime. This requires a more accurate calculation of the ground PES, obtainable with a finer mesh.

3. RESULTS

3.1 Ground PES

We first consider the ground PES. To obtain converged results for equilibrium nuclear positions and vibrational frequencies, we found it necessary to use mesh spacing of $\Delta x = 0.2$ Å. The orbital wave functions are defined on the grid points that lie within a sphere. We found that a sphere of radius $R = 5$ Å is adequate to obtain converged ground orbital energies. Some properties related to the ground PES are shown in Table 1. The C–C equilibrium distance is reproduced to 1% accuracy. The curvature of the potential energy surface for the two important modes, the C–C stretch and the torsion, control the respective vibrational frequencies. As may be seen from the Table, the empirical vibrational frequencies[13] are reproduced to about 5% accuracy. We also quote the results of the ab initio calculations of refs 14 and 5, which show more or less the same accuracy. We conclude that the quality of the DFT results are encouraging to proceed with the calculation of anharmonic and large amplitude fluctuation effects.

3.2 Vertical Excitations

Next we turn to the TDDFT excitation energies at the equilibrium geometry (called the Franck–Condon point, FCP). The TDDFT predictions with the LDA energy functional are shown in Table 2. The π–π* transition appears at 7.5 eV excitation energy with an oscillator strength of $f = 0.30$. This energy is about 0.2 eV lower that the center of gravity of the observed peak. Also, comparing to the measured strength of 0.42 in this region, we infer that additional electronic transitions are likely to be present. Indeed, the TDDFT produces other states in the same region of excitation. The three additional states have a Rydberg character with diffuse orbitals. Only the lowest of these, which is *s*-like and has no angular nodes at large distance, is optically active. It has a transition strength of $f = 0.08$. Adding this to the π–π* strength, the total strength is only 0.04 units below the observed value. We note that our oscillator strengths are quite close to those obtained by quantum chemistry methods, e.g., ref 5. In principle, the LDA cannot give reliable excitation energies for the Rydberg states, due to an incorrect asypmtotic potential. However, the present results are within 0.3 eV of the more refined theoretical values in the last column. It might be possible to improve the energies by using a GGA density-functional as in ref 16, but for the present study we will use the LDA and confine our attention to the π–π* transition.

Table 1. Ground-state properties of ethylene

	experimental	DFT	refs 6,14	ref 5
R_{CC} Å	1.339	1.335	1.347	
ω_{CC} (eV)	0.201	0.19	0.21	0.22
$\omega_{torsion}$ (eV)	0.127	0.12	0.134	0.135

Table 2. Calculated electronic excitations in ethylene at the FCP. The lowest 4 excitations are mainly configurations made by exciting a π-electron to the π* or to a Rydberg orbital. We follow the convention used by ref 13 for the *x, y, z* axes

excited orbital	ω (LDA)	f (LDA)	ref 5	ref 14
s-Rydberg	6.8	0.08	7.3,0.08	6.8
p_x-Rydberg	7.3	0		7.5
p_y-Rydberg	7.4	0		7.5
π*	7.5 eV	0.30	8.1,0.36	7.8

3.3 Coupling to the Nuclear Coordinates

The nuclear coordinates that have the largest effect on the transition are the C–C stretch coordinate and the torsion angle coordinate. We shall consider both of these in the sections below. The CH_2 wagging coordinates also play a role, first in mixing the π–π* excitation with Rydberg excitations,[4,17] and then at large torsion angles providing a direct path from the excited PES to the ground PES.[6] Since we ignore the Rydberg states and do not treat the multidimensional character of the nuclear coordinate space at all, we shall neglect the wagging and other modes that couple indirectly.

3.3.1 C–C stretch motion

Historically, the first candidate for the source of the width of the π–π* transition was the coupling to the C–C stretch coordinate. Calculating the excited PES along the stretch coordinate according to eq 2, we find the results shown in Fig. 1. The excited PES has a minimum at $R_{CC} = 1.5$ Å with an energy 7.0 eV. The slope of the PES at the FCP is given by $dE_{ex}/dQ = 8$ eV/Å. This is all we need to estimate the width using eq 4. Taking $\sigma_Q = 0.04$ Å from empirical vibrational frequency, we find a variance of $\sigma_E \approx 0.3$ eV for the absorption peak. The corresponding width is $\Gamma = 0.7$ eV, roughly 2/3 of the observed peak width. We expect that the widths from fluctuation of different coordinates add in quadrature. Thus, the width due to fluctuation in the C–C distance must be augmented by a similar width from other coordinates.

The observed peak has an apparent asymmetry, falling off more steeply on the low-energy side. In principle, the asymmetry can be calculated using the full expression eq 3. We first solve the Schroedinger equation on the ground PES to get the wave function $\Psi(Q)$, and then apply eq 3 directly. The result is shown in Fig. 2.

p_x 7.8 p_y 7.3
p_z 7.4

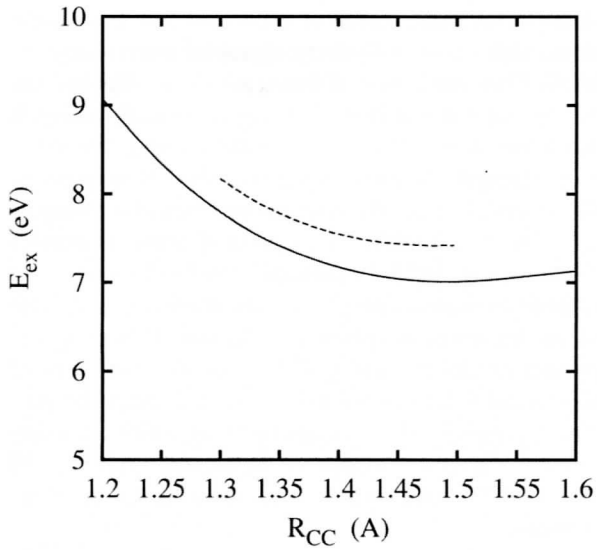

Fig. 1. Excited PES along the C–C stretch coordinate. Solid: TDDFT; dashed: ref 6.

Indeed, a significant asymmetry is predicted, reflecting the anharmonicity in the ground PES and the curvature of the excited PES. However the width is still too small. We mention that the calculation of ref 14 also predicts an asymmetric peak. Their width includes all the vibrational modes, and comes out somewhat larger than the observed width.

3.3.2 Coupling to torsional motion

Experimentally, the strong absorption peak at 7–8 eV has a progression of strength at low energies, seen down to nearly 6 eV.[19] The C–C stretch PES doesn't drop to that low an energy, leaving the torsional mode as the most likely source of the strength. Combining the inertia I_θ (with $\hbar^2/I_\theta \approx 0.0048$ eV/r^2) of the torsional motion with empirical vibrational frequency $\omega_{torsion}$, the zero-point fluctuation variance in the torsional angle is given by $\langle\theta^2\rangle^{1/2} = \sqrt{\hbar/2I_\theta\omega_{torsion}} \approx 8°$. This is rather soft, and suggests that coupling to this coordinate could be significant. Unfortunately, the π–π* excitation mixes with the Rydberg states at finite torsional angles,[4,17] splitting the original π–π* transition into several components. Since the Rydberg excitation energies are not accurate in the LDA, we choose to ignore the splitting of the π–π* state, taking the diabatic state at the mean excitation energy associated with an excitation along the x coordinate. The diabatic excited PES is shown in Fig. 3. Using it in eq 3, we obtain the strength distribution shown in Fig. 4. Qualitatively the measured fall-off is reproduced, but in detail the predictions are not as accurate as we had found for the forbidden transitions in benzene. In the region of 6.5–7.0 eV, the theoretical strength is too high, by about a factor of three. The agreement is much better at lower energies, down to 6.1 eV, the lowest energy measured in ref 19. However, the theory should be more reliable the closer to the FCP, so the low energy agreement is probably a fortuitous cancellation of opposite-sign errors.

A likely cause of the discrepancy just below 7 eV is the error in the TDDFT excitation energy. In Fig. 2, we saw that the strength around the main peak in the LDA calculation is somewhat lower than the observed one. This is within a typical error of the TDDFT for excitation energy. An overall shift of 0.2 eV in the excited state PES would improve the description of strength function both in the peak region and in the region as far

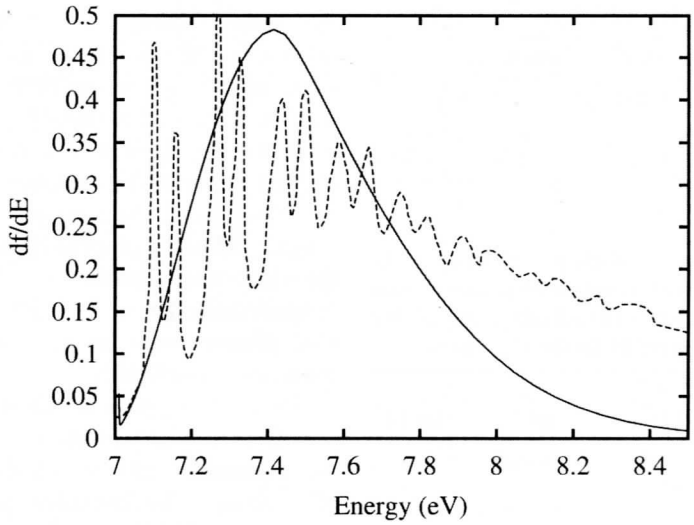

Fig. 2. Line broadening of the π–π* excitation due to the zero-point motion in the C–C bond coordinate. Solid: TDDFT theory; dashed: experimental.[13]

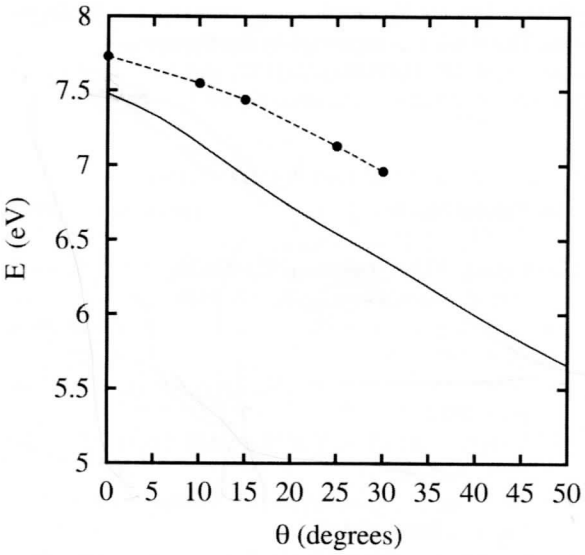

Fig. 3. Excited PES along the torsional coordinate. The solid line is the TDDFT result with other coordinates fixed at the FCP. The dashed line is from ref 18.

down as 6.5 eV. Shifting the excited state PES in that way, on the other hand, would destroy the present agreement below 6.5 eV. However, this large-angle region of PES is only accessible by a deep tunneling of the nuclear motion. It might be that the naive reflection treatment becomes inaccurate. For example, it might be that the tunneling in the excited state vibrational wave function becomes important. It may also be that thermally promoted tunneling on the ground PES becomes significant in the deep tunneling region, even though the thermal excitation probabilities are small. However, we leave it for future work to investigate these possibilities.

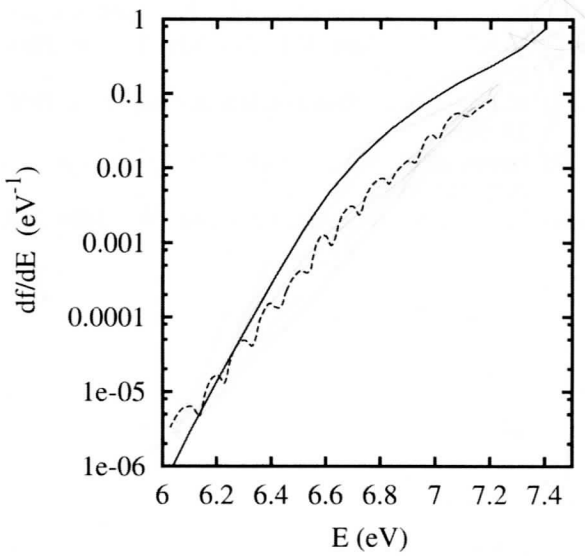

Fig. 4. Low energy absorption strength associated with the zero-point motion in the torsional coordinate. Solid: present theory; dashed: experiment.[19]

4. DYNAMICS ON THE EXCITED PES

We now discuss briefly nuclear dynamics on our excited PES. An interesting measurement of a dynamic timescale on the excited PES was reported in ref 20, made by a two-photon pump-probe technique. In the experiment the two photon energies were 6.2 eV and 4.64 eV, and the average time delay between them could be varied. The ionization rate was measured as a function of the delay time. The observed ionization yield peaked when the pulse associated with the lower energy photon was delayed by about 50 fs from the pulse of the more energetic photon. Clearly, the ethylene must first be excited by the 6.2-eV photon before it can absorb the lower energy photon. The experiment was interpreted in terms of lifetime of the state excited by the 6.2-eV photon, with an extracted value of 30 ± 15 fs. The ionization threshold of ethylene is 10.5 eV, so the total energy available is only 0.3 eV above the threshold.

While the complete dynamics on the excited state PES are beyond the TDDFT, the PES we have already constructed can be used to estimate the accelerations in the short-time domain after excitation. According to the calculation in the previous section, the absorption strength at 6.2 eV comes from the torsional zero-point fluctuation of the hydrogens rotated to an angle of about 35°. Let us assume that the ionization potential of the molecule is independent of the angle. Then, as long as the excitation energy is kept in the electronic degrees of freedom, the ionization can take place. However, the gradient in the PES will cause an acceleration in that coordinate, converting energy from potential to kinetic. The kinetic energy associated with nuclear motion cannot be used in the ionization process, so these accelerations give the first quenching of the ionization rate. To make a concrete estimate, we use the slope of the TDDFT PES to determine the acceleration. At 35°, the PES is still rapidly falling, with a slope given by $dE_{ex}/d\theta \approx 2$ eV/rad^2. Taking this as the force in Newton's equation, the system acquires an angular velocity given by

$$\frac{d\theta}{dt} = \frac{1}{I_\theta}\frac{dE_{ex}}{d\theta}t$$

with a corresponding kinetic energy

$$K = \frac{1}{2}I_\theta\left(\frac{d\theta}{dt}\right)^2.$$

Evaluating these expression numerically, we find that it only takes 5 fs for the kinetic energy to grow to 0.5 eV. This would put the potential energy below the ionization threshold, and indicates that the quenching should happen very rapidly.

However, the fact that vibronic structure is seen in the strength function tells one that the motion along the torsional coordinate is not very dissipative. The system can accelerate to a very large angle, bounce, and return to a state with no kinetic energy in the nuclear motion. Since we cannot say what the true irreversible rates are, the considerations here can only give a lower bound on the effects of a time delay. We note that the calculation of ref 6 treats the large-angle motion as well and obtains results consistent with the observed time correlation.

5. CONCLUSIONS

In this article, we aimed to elucidate how well the TDDFT works in describing electron–nucleus coupling. For this purpose, we analyzed the π–π^* transition of the ethylene molecule in the 6–8-eV region. The DFT and TDDFT were employed to construct the ground and excited PES in the LDA. A simplified treatment in the reflection approximation is made for the Frank–Condon factor. The TDDFT describes reasonably well the vertical excitation energy and the magnitude of oscillator strength. The roles of the C–C stretch motion and the torsional motion on the spectral line shape were investigated. We found that the C–C stretch coordinate contributes substantially to the width of the transition, but the torsional coordinate is responsible for the low energy tail. There the transition strength is reproduced by about a factor of three, over 4 orders of magnitude. We thus conclude that the TDDFT survives the first tests as a useful approximation to treat electron–nucleus couplings in excited states. As next steps, a more sophisticated treatment of the quantum nuclear motion would be required, as well as an improved treatment of the exchange-correlation potential beyond the LDA.

Acknowledgments. We thank T.J. Martinez for helpful discussions. This work was supported by the Department of Energy under Grant DE-FG03-00-ER41132, and facilitated by the Computational Materials Science Network.

REFERENCES AND NOTES

(1) Yabana, K.; Bertsch, G.F. *Int. J. Quant. Chem.* **1999**, *75*, 55.
(2) Casida, M.E.; Jamorski, C.; Casida, K.C.; Salahub, D.R. *J. Chem. Phys.* **1998**, *108*, 4439.
(3) Bertsch, G.F.; Schnell, A.; Yabana, K. *J. Chem. Phys.* **2001**, *115*, 4051.
(4) Petrongolo, C.; Buenker, R.; Peyerimhoff, S. *J. Chem. Phys.* **1982**, *76*, 3655.
(5) Mebel, A.M.; Chen, Y.T.; Lin, S.H. *Chem. Phys. Lett.* **1996**, *258*, 58.
(6) Ben-Nun, M.; Quenneville, J.; Martinez, T.J. *J. Phys. Chem. A* **2000**, *104*, 5161.
(7) Cooper, G.; Olney, T.N.; Brion, C.E. *Chem. Phys.* **1995**, *194*, 175.
(8) Perdew, J.P.; Zunger, A. *Phys. Rev. B* **1981**, *23*, 5048.
(9) Heller, E.J. *J. Chem. Phys.* **1978**, *68*, 2066.
(10) Boisseau, C.; Audouard, E.; Vigue, J.; Julienne, P.S. *Phys. Rev. A* **2000**, *62*, 052705.
(11) Troullier, N.; Martins, J. *Phys. Rev. B* **1991**, *B43*, 1993.
(12) Kleinman, L.; Bylander, D. *Phys. Rev. Lett.* **1982**, *48*, 1425.
(13) Sension, R.J.; Hudson, B.S. *J. Chem. Phys.* **1989**, *90*, 1377.
(14) Ben-Nun, M.; Martinez, T.J. *J. Phys. Chem.* **1999**, *103*, 10517.
(15) van Leeuwen, R.; Baerends, E.J. *Phys. Rev. A* **1994**, *49*, 2421.
(16) Nakatsukasa, T.; Yabana, K. *J. Chem. Phys.* **2001**, *114*, 2550.
(17) Ryu, J.; Hudson, B.S. *Chem. Phys. Lett.* **1995**, *245*, 448.
(18) Mebel, A.M.; Chen, Y.T.; Lin, S.H. *J. Chem. Phys.* **1996**, *105*, 9007.
(19) Wilkinson, P.G.; Mulliken, R.S. *J. Chem. Phys.* **1955**, *23*, 1895.
(20) Farmanara, P.; Stert, V.; Radloff, W. *Chem. Phys. Lett.* **1998**, *288*, 518.
(21) Ben-Nun, M.; Martinez, T.J. *Chem. Phys.* **2000**, *259*, 237.